Regulation of G_i by the CB_1 Cannabinoid Receptor C-Terminal Juxtamembrane Region: Structural Requirements Determined by Peptide Analysis†

Somnath Mukhopadhyay,‡ Sudha M. Cowsik,‡,§,|| Andrew M. Lynn,|| William J. Welsh,§ and Allyn C. Howlett*,‡

Department of Pharmacological and Physiological Science, Saint Louis University School of Medicine, St. Louis, Missouri 63104, Department of Chemistry and Center for Molecular Electronics, University of Missouri−St. Louis, St. Louis, Missouri 63121, and School of Life Sciences, Jawaharlal Nehru University, New Delhi 110067, India

Received July 22, 1998; Revised Manuscript Received January 4, 1999

ABSTRACT: A CB_1 cannabinoid receptor peptide fragment from the C-terminal juxtamembrane region autonomously inhibits adenylyl cyclase activity in a neuroblastoma membrane preparation. The cannabinoid receptor antagonist, SR141716A, failed to block the response. The peptide was able to evoke the response in membranes from Chinese hamster ovary (CHO) cells that do not express the CB_1 receptor. These studies are consistent with a direct activation of G_i by the peptide. To test the importance of a BXBXXB sequence, Lys_{403} was acetylated, resulting in a peptide having similar affinity but reduced efficacy. N-Terminal truncation of Arg_{401} resulted in a 6-fold loss of affinity, which was not further reduced by sequential truncation of up to the first seven amino acids, four of which are charged. N-Terminal-truncated peptides exhibited maximal activity, suggesting that G_i activation can be conferred by the remaining amino acids. Truncation of the C-terminal Glu_{417} or substitution of Glu_{417} by a Leu or of Arg_{401} by a Norleucine reduced activity at 100 μM. The C-terminal juxtamembrane peptide was constrained to a loop peptide by placement of Cys residues at both terminals and disulfide coupling. This modification reduced the affinity 3-fold but yielded near-maximal efficacy. Blocking the Cys termini resulted in a loss of efficacy. Circular dichroism spectropolarimetry revealed that all C-terminal juxtamembrane peptide analogues exist in a random coil conformation in an aqueous environment. A hydrophobic environment (trifluoroethanol) failed to induce α-helix formation in the C-terminal juxtamembrane peptide but did so in less active peptides. The anionic detergent sodium dodecyl sulfate induced α-helix formation in all analogues except the loop peptide, where it induces a left-handed PII conformation. It is concluded that α-helix formation is not required for G_i activation.

The CB_1 cannabinoid receptor is a member of the G-protein coupled receptor family that interacts with the pertussis toxin-sensitive $G_{i/o}$ family of G-proteins to inhibit adenylyl cyclase (*1*, *2*), regulate N-type Ca^{2+} channels (*3*), and initiate the mitogen-activated protein kinase pathway leading to immediate early gene induction (*4*). The amino acid sequence determined for the CB_1 cannabinoid receptor is 97% conserved in human, rat, and mice (*5*−*8*). The primary structure is consistent with the seven transmembrane helical structure that characterizes G-protein coupled receptors. Bramblett et al. (*9*) analyzed the secondary structure of the CB_1 receptor based upon hydrophobicity and a variability profile to predict the regions of α-helicity. Using the Bramblett alignment as a guide, we explored the intracellular loop regions of the CB_1 receptor for their ability to interact with G-proteins in in vitro studies using peptides and site-directed antibodies (*10*). We found that peptide fragments from the N-terminal side of the third intracellular loop and the C-terminal juxtamembrane region autonomously inhibited adenylyl cyclase activity. This would suggest that these peptides represent two domains on the receptor that interact with and contribute to the activation of G_i.

The synthetic peptide fragment of the C-terminal juxtamembrane region ($CB_1$401−417) has been previously shown to activate G-proteins autonomously by its ability to promote [^{35}S]GTPγS binding to G-proteins in brain membranes (predominantly G_o). $CB_1$401−417 activates G_i in neuroblastoma membranes to inhibit adenylyl cyclase, and this response can be blocked by pertussis toxin treatment, suggesting that the peptide−G_i interaction is compromised by ADP-ribosylation as is the receptor−G_i interaction (*11*). In the present study, we have used peptide $CB_1$401−417 to analyze the structural requirements important for optimal activation of G_i by this domain of the receptor. We have provided evidence that activation by peptide is not dependent on receptor activation, implicating a peptide−G_i interaction. We have examined a series of peptide analogues for their ability to activate G_i and for conformation in various environments monitored by CD[1] spectroscopy. The data indicate that α-helix-forming ability is not required for activation of G_i by these peptides.

† This work was supported by National Institute on Drug Abuse Grants R01-DA03690 and K05-DA00182. Production of CB_1-CHO cells was supported in part by P01-DA09158.

* To whom correspondence should be addressed: Department of Pharmacological and Physiological Science, Saint Louis University School of Medicine, 1402 South Grand Blvd., St. Louis, MO 63104.

‡ Saint Louis University School of Medicine.

§ University of Missouri−St. Louis.

|| Jawaharlal Nehru University.

10.1021/bi981767v CCC: $18.00
Published on Web 02/19/1999

Table 1: CB_1 Cannabinoid Receptor Peptide Fragments

Peptide	Sequence	Notation
$CB_1$401-417[a]	RSKDLRHAFRSMFPSSE	C-terminus(juxtamembrane)
Acetyl-*lys*$_{403}$-$CB_1$401-417	RSKDLRHAFRSMFPSSE └Ac	C-terminus(juxtamembrane)
$CB_1$402-417	_SKDLRHAFRSMFPSSE	N-truncated sans (+)
$CB_1$404-417	___DLRHAFRSMFPSSE	N-truncated sans (+)(OH)(+)
$CB_1$406-417	_____RHAFRSMFPSSE	N-truncated sans (+)(OH)(+)(-)
$CB_1$408-417	_______AFRSMFPSSE	N-truncated sans (+)(OH)(+)(-)(+)
CB_1nor*leu*402-417	nLSKDLRHAFRSMFPSSE	N-side (+) neutralized
$CB_1$401-416*leu*	RSKDLRHAFRSMFPSSL	C-side (-) neutralized
$CB_1$401-415	RSKDLRHAFRSMFPS__	C-side truncated sans *(cys)*(-)
CB_1*cys*401-415*cys* (disulfide)	CRSKDLRHAFRSMFPSC └──────────┘	Structure constrained by disulfide linkage at ends
CB_1*cys*(acm)401-415*cys*(acm)[b]	CRSKDLRHAFRSMFPSC └Acm └Acm	Free conformation blocked at sulfhydrils

[a] The numbers correspond to inclusive amino acids (*6*). *Ser* replaced a Cys in the sequence to avoid spontaneous disulfide formation in solution. [b] acm is the acetamido sulfhydryl blocking group.

EXPERIMENTAL PROCEDURES

Peptide Synthesis. Peptides described in Table 1 were synthesized by fluoromethoxycarbonyl chemistry and purified over a Microsorb C-18 reverse-phase HPLC column by Princeton Biomolecules (Columbus, OH). The structures of the peptides were verified by GC/MS at Princeton Biomolecules. The amino acid sequences of peptides $CB_1$401−417 and acetyl-Lys$_{403}$−$CB_1$401−417 were verified by automated Edman degradation at the Saint Louis University Peptide Facility.

Acetylation of Peptide CB_1 401−417. The Lys$_{403}$ was acetylated following a modification of the method of Shen and Strobel (*12*). The peptide was dissolved in water (2 mg/mL), followed by addition of an equal volume of saturated sodium acetate (15 M). Acetic anhydride was slowly added to a final concentration of 6 mM and the reaction mixture was continuously stirred at 0−4 °C for 1 h. The reaction was stopped by lyophilization, and the lyophilized powder was dialyzed overnight against water. The purity of the modified peptide was checked by HPLC, performed on a Varian Star Workstation (9095 autosampler, 9010 solvent delivery system, 9050 UV detector, and Microsorb M−V C18 column). The mobile phase comprised solvent A, 0.1% TFA, and solvent B, 80% acetonitrile and 0.085% TFA; all solvents were filtered and degassed prior to use. The elution program was as follows: 0 min, 100% solvent A; 5 min, 80% solvent A and 20% solvent B; 40 min, 20% solvent A and 80% solvent B; 45 min, 100% solvent B. Absorbance was measured at 214 nm. The control peptide eluted at 21.4 min and the acetylated peptide eluted at 20.6 min. A mixture of both control and acetylated peptide eluted at the same times as the individual peaks.

Membrane Preparation and Adenylyl Cyclase Assay. N18TG2 cell membranes were prepared and adenylyl cyclase assays were carried out as described (*1*). CHO cells and CB_1−CHO cells stably expressing exogenous CB_1 cannabinoid receptors were a gift from Dr. D. A. Kendall, University of Connecticut (*13*), and were grown in Dulbecco's modified Eagle's/Ham's F12 (1/1) medium supplemented with 10% heat-inactivated calf serum plus 50 IU/mL penicillin and 50 μg/mL streptomycin. Plasma membrane fractions were prepared by nitrogen cavitation disruption and density gradient sedimentation exactly as described for the N18TG2 cells (1). The adenylyl cyclase reaction mixture included membranes (15 μg of protein), forskolin (10 μM), and Ro20−1724 (100 μM) [plus isobutylmethylxanthine (100 μM) for CB_1−CHO membranes]. The concentrations of fatty acid-free BSA present in these enzyme assays were 0.16−0.21 mg/mL. The forskolin-stimulated enzyme activities from these studies averaged 83.4 ± 3.03 pmol min^{-1} (mg of protein)$^{-1}$ (mean ± SEM, $n = 18$). Triplicate determinations were made for each data point, and data are presented as the percent inhibition of forskolin-stimulated adenylyl cyclase activity. Data were analyzed by ANOVA followed by the Bonferroni posthoc test.

Circular Dichroism Studies of Peptides. The CD spectra were measured on a Jasco J-500 or J-720 spectropolarimeter. Peptide samples for CD measurements were approximately 75 μM. The instruments were calibrated with 0.06% ammonia d-10-camphorsulfonate. Spectra were acquired at ambient temperature (298 K) over 190−240 nm using a 1.0 mm quartz cuvette at a sensitivity of 2.0 mdeg/cm and a scan speed of 20 nm/min. Spectra were recorded digitally and each signal was averaged from 4 runs followed by subtracting a similarly signal-averaged solvent baseline. To mimic different biomembrane compartments, different solvents were used. The aqueous compartment was mimicked

[1] Abbreviations: BSA, bovine serum albumin; CD, circular dichroism; CHO, Chinese hamster ovary fibroblasts; DALN, desacetyllevonantradol; DPPG, dipalmitoylphosphatidylglycerol; GC/MS, gas chromatography/mass spectrometry; HPLC, high-performance liquid chromatography; SDS, sodium dodecyl sulfate; TFA, trifluoroacetic acid; TFE, trifluoroethanol.

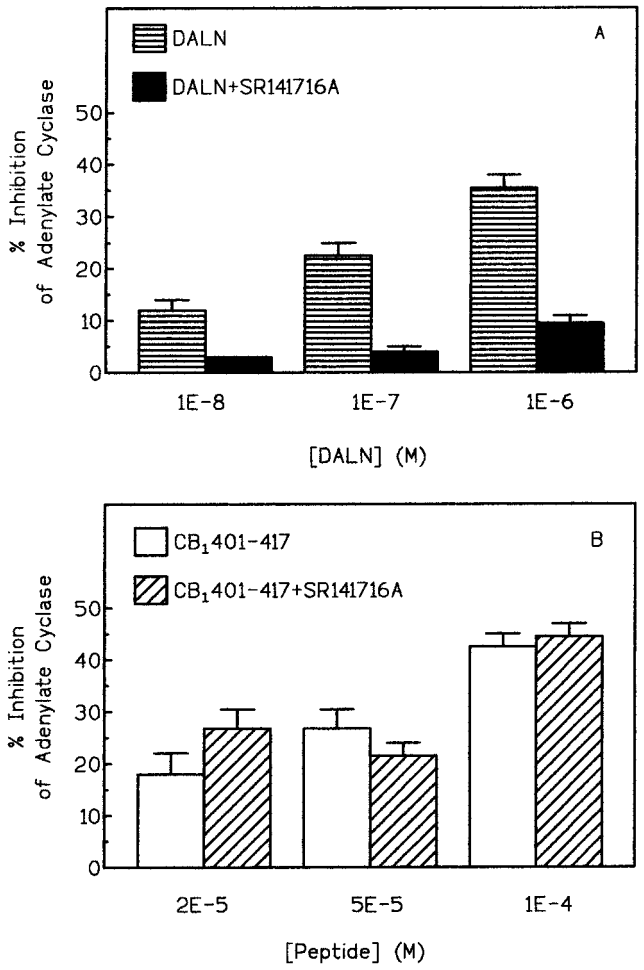

FIGURE 1: Effect of antagonist SR141716A on the DALN- and $CB_1$401−417- mediated inhibition of adenylyl cyclase activity. DALN (A) or peptide $CB_1$401−417 (B) was included in the reaction mixture at the indicated concentrations in the presence and absence of SR141716A (1 μM). Data are presented as mean ± SEM of three independent experiments. (A) Inhibition of adenylyl cyclase was significantly different ($p < 0.05$) between the absence (striped bar) and presence (solid bar) of SR141716A at all DALN concentrations. (B) No significant difference ($p < 0.05$) was observed between the absence (open bar) and presence (hatched bar) of SR141716A at any of the peptide concentrations.

by a 10 mM sodium phosphate buffer at pH 7.2, the charged surface by the anionic detergent SDS, and the hydrophobic membrane interior by TFE. CD spectra for all peptides were recorded in water, sodium phosphate buffer, and increasing concentrations (vol/vol) of TFE, methanol, anionic detergent SDS, and anionic lipid DPPG (45 μM) micelles.

RESULTS

Activation of G_i by Peptide CB_1 401−417 Bypasses the CB_1 Receptor. Two studies were performed to support the contention that the C-terminal juxtamembrane fragment peptide $CB_1$401−417 can directly activate the G_i protein. An experiment was performed to demonstrate that inhibition of the receptor by the competitive antagonist SR141716A (*14*) fails to alter the response to the C-terminal juxtamembrane peptide. Inhibition of adenylyl cyclase was elicited by the CB_1 cannabinoid receptor agonist DALN, increasing to the maximally effective 1 μM. This response was blocked by 1 μM SR141716A, as shown in Figure 1A. However,

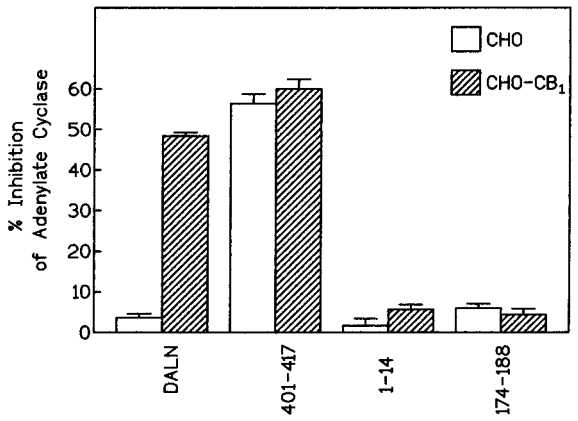

FIGURE 2: Effect of agonist DALN and peptide $CB_1$401−417 on inhibition of adenylyl cyclase activity in membranes from CHO and CB_1 −CHO cell membranes. DALN (1 μM) or peptides CB_1-401−417, $CB_1$1−14, or $CB_1$174−188 (100 μM) were included in the adenylyl cyclase reaction mixture. Data are from two independent experiments. The effect of DALN in CB_1−CHO membranes was significantly different from its effect in CHO membranes ($p < 0.05$). No significant difference ($p < 0.05$) between the CB_1−CHO and CHO membranes was observed for any of the peptides.

SR141716A failed to attenuate the response to submaximal or maximally effective concentrations of peptide $CB_1$401−417 (Figure 1B). This study demonstrates that the response to the juxtamembrane C-terminal peptide fragment does not act by mimicking the agonist at the receptor.

To confirm that the G-protein activating capability of the peptide does not depend on the presence of the CB_1 receptor, adenylyl cyclase activity was determined in membranes from CHO and CB_1−CHO cells (*13*). The CB_1 receptor agonist DALN was active only in the membranes from CB_1−CHO cells, demonstrating that this agonist acts via the expressed human CB_1 receptor (Figure 2). Peptide $CB_1$401−417 activated G_i to inhibit adenylyl cyclase activity both in cells expressing the CB_1 receptor and in the wild-type CHO cells, which are devoid of cannabinoid receptors. As controls to demonstrate specificity of peptide $CB_1$401−417 to evoke G_i activation, fragments from the N-terminus (amino acids 1−14) and from the first extracellular loop of the CB_1 receptor (amino acids 174−188) were also tested in the adenylyl cyclase assay (*10*). Neither of these peptides resulted in inhibition of adenylyl cyclase at the concentration of CB_1-401−417 that produced a maximal response (100 μM).

Determination of Functionally Critical Amino Acids of CB_1 401−417 Peptide. The efficacy of the CB_1 receptor juxtamembrane C-terminal peptide to activate G_i suggests that a conformation of the isolated peptide fragment can be adopted that is able to mimic the receptor conformation. There are three Arg and one Lys nonconsecutive residues within the N-terminal-side sequence of the CB_1 C-terminal peptide, posing the possibility for a cationic patch. For a number of G-protein coupled receptors, a motif of BBXXB or BBXB (where B is a basic residue and X is any amino acid) has been proposed to be present on the N-terminal sides of intracellular loops that couple to G-proteins (*15*, *16*). The CB_1 receptor C-terminal juxtamembrane peptide possesses a modification of such a motif (BXBAXB, where A is an acidic residue). To determine the importance of this motif to peptide $CB_1$401−417, the sequence of discontinuous positive charges was disrupted by neutralization of the

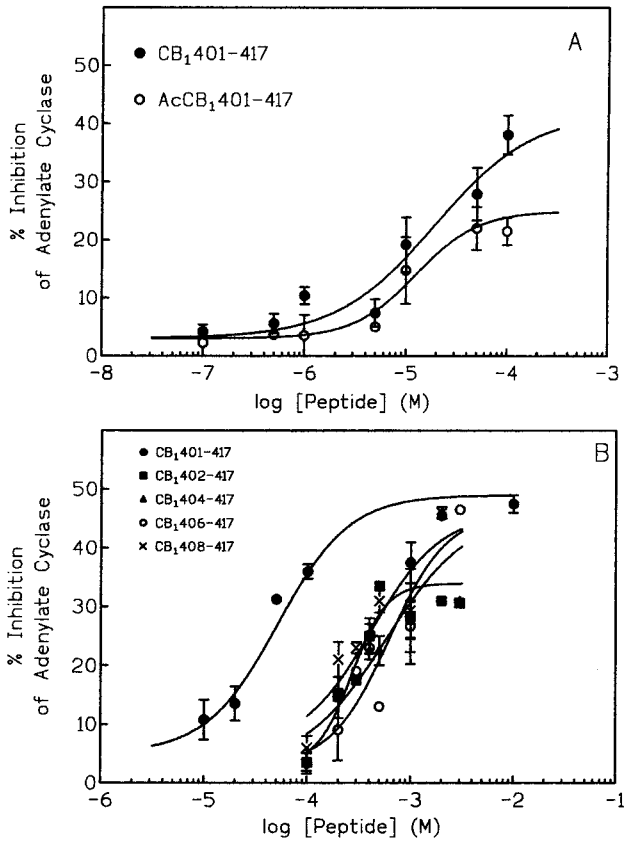

FIGURE 3: (A) Effect of Lys_{403} acetylation of $CB_1401-417$ on inhibition of adenylyl cyclase activity. $CB_1401-417$ and acetyl-$Lys_{403}-CB_1401-417$ ($AcCB_1401-417$) were present in the incubation mixture at the indicated concentrations and data are expressed as the percent inhibition promoted by the peptides. Each bar depicts mean ± SEM of three separate experiments. The curves were analyzed by Graphpad Inplot for nonlinear regression analysis of a sigmoidal curve in which maxima, minima, concentration at half-maximal activity, and slope were unconstrained. (B) Dose−response effect of N-terminal-side truncated $CB_1401-417$ peptide analogues on inhibition of adenylyl cyclase activity. Data (mean ± SEM) are from two separate experiments. Curves were analyzed for nonlinear regression analysis of sigmoidal curves by Graphpad Inplot. For peptides $CB_1401-417$ and $CB_1402-417$, for which maximal activities were achieved for at least 1 order of magnitude in the experimental points, all parameters were unconstrained. However, because the shapes of the curves of the other peptides were not obviously sigmoidal with the points available, these curves were constrained at a maximum defined by the highest peptide concentration tested (3 mM), which was also the maximum for $CB_1401-417$. For these curves, the EC_{50} values should be considered theoretical.

intervening Lys_{403} through acetylation. The resulting BXX-AXB pattern would be expected to present a very different charge patch surface to the G-protein. The acetylated peptide was found to retain the G_i activation response. However, this modification resulted in a loss in the maximal activity, being reduced from 42% to 22% inhibition of adenylyl cyclase at 100 μM (Figure 3A). Concentrations of acetyl-$Lys_{403}-CB_1401-417$ as high as 1 mM failed to evoke inhibition of adenylyl cyclase greater than 25% (data not shown). Peptide $CB_1401-417$ exhibited an EC_{50} of 32 μM, whereas acetyl-$Lys_{403}-CB_1401-417$ exhibited a somewhat lower EC_{50} at 13 μM. Thus, disruption of the multibasic BXBAXB motif appears to result in a peptide that is active with reduced efficacy but exhibits a similar apparent affinity for the G-protein.

In an attempt to determine whether the N-terminal-side positive charges of the peptide $CB_1401-417$ comprise a functional motif for interaction with G-proteins, peptides with serial removal of one or two amino acids from the N-terminal side were tested for inhibition of adenylyl cyclase activity (Figure 3B). Removal of Arg_{401} in peptide $CB_1402-417$ resulted in almost total loss of the inhibitory effect of the peptide on adenylyl cyclase activity at 100 μM concentration. This was due to a loss of apparent affinity, inasmuch as the EC_{50} exhibited by $CB_1402-417$ was 226 μM compared with 45 μM for the nontruncated $CB_1401-417$. This Arg_{401}-truncated peptide was also less efficacious, inhibiting adenylyl cyclase by only 31% compared with 42% for the nontruncated peptide. When 100 μM $CB_1402-417$ (4% inhibition) was combined with 100 μM $CB_1401-417$ (32% inhibition), an intermediate value (16% inhibition) was obtained (data not shown). This might suggest that $CB_1402-417$ could compete for access to the G-protein but not evoke the full response, in a manner reminiscent of a partial agonist. Further truncation on the N-terminal side as in peptides $CB_1404-417$, $CB_1406-417$, and $CB_1408-417$ evoked inhibition of adenylyl cyclase to the same maximal extent as did $CB_1402-417$ when the peptides were tested at >1 mM. Caution is generally exercised in interpretation of data at such high peptide concentrations; however, it should be noted that extending the concentration of peptide $CB_1401-417$ from 100 μM to 10 mM did not result in any aberrancy in the log dose−response curve. The EC_{50} values were estimated to be 631 μM, 649 μM, and 810 μM for peptides $CB_1404-417$, $CB_1406-417$, and $CB_1408-417$, respectively, applying the constraint that the maximal response occurred at the 3 mM concentration of each peptide. Addition of inactive (100 μM) concentrations of these N-terminal-truncated peptides to 100 μM $CB_1401-417$ or 1 μM DALN did not significantly alter the effect on adenylyl cyclase activity (data not shown), implying that these peptides did not behave as competitive antagonists. These data would suggest that the residue of primary importance in determining apparent affinity for the G-protein was Arg_{401}.

The importance of the positive charge on the N-terminal residue for G-protein activation was tested by substitution of uncharged amino acid norleucine (Nle) (having almost the same bulk) for Arg_{401} in peptide $CB_1Nle402-417$. As shown in Figure 4, 100 μM $CB_1401-417$ exhibited 37% inhibition of adenylyl cyclase in this set of experiments, whereas $CB_1Nle402-417$ exhibited only 8% inhibition at the same concentration. This loss of activity is believed to be due to a loss of efficacy because increasing the concentration to as high as 1 mM failed to evoke any greater inhibition of adenylyl cyclase (data not shown).

To further explore the importance of negatively charged Glu_{417}, two peptide analogues were synthesized by truncation at the C-terminal side ($CB_1401-415$) or substitution of the negatively charged Glu with a Leu ($CB_1401-416Leu$). Removal of the C-terminal two amino acids from $CB_1401-417$ rendered poor activity (7% inhibition of adenylyl cyclase) when tested at 100 μM (Figure 4). The peptide $CB_1401-416Leu$, however, inhibited the enzyme activity 13% to 21.5% going from 10 μM to 100 μM. It was not possible to achieve graduated log dose−response curves with these peptides that had been modified to uncharged residues at the terminals. It might be postulated that the elimination of

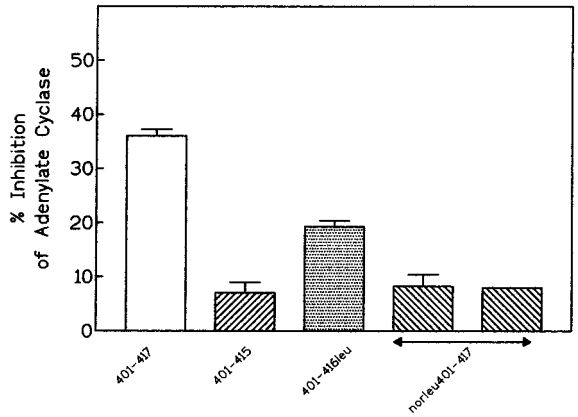

FIGURE 4: Effect of CB_1Nle402−417, $CB_1$401−415, and $CB_1$401−416Leu on inhibition of adenylyl cyclase activity. Peptides were included in the reaction mixture at 100 μM or 100 μM and 1 mM for CB_1Nle402−417. Data are mean ± SEM from three separate experiments. The activities of peptides $CB_1$401−415 and $CB_1$401−416Leu were significantly lower than that of $CB_1$401−417 ($p < 0.05$).

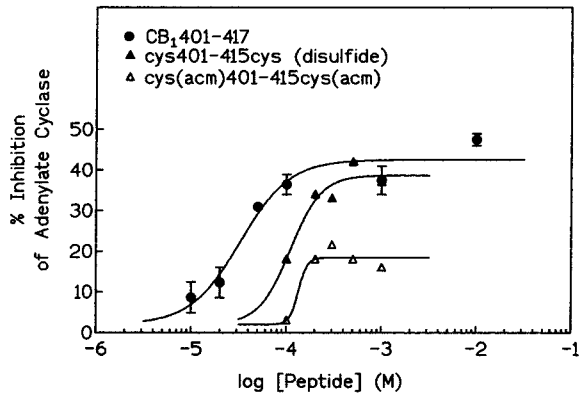

FIGURE 5: Dose−response effect of loop peptide CB_1Cys401−415Cys (disulfide) and its control CB_1 Cys(acm)401−415Cys(acm) on inhibition of adenylyl cyclase activity. Data are the average and range from two separate experiments.

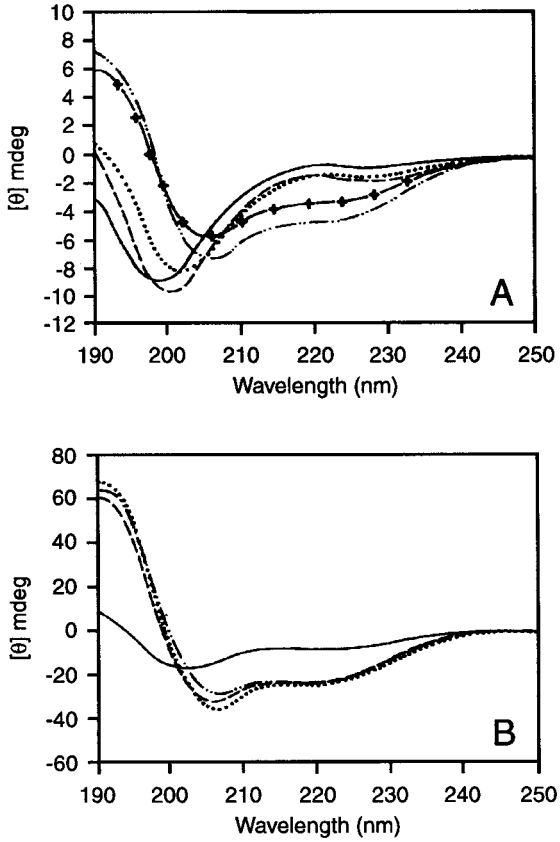

FIGURE 6: CD spectra for (A) $CB_1$401−417 compared with (B) mastoparan. Solvents for the peptides were: (—) 10 mM sodium phosphate, pH 7.2; (···) 100% methanol; (— — —) 80% TFE in panel A and 20% TFE in panel B; (+) 0.1% SDS; (— ·· —) 1.0% SDS.

the terminal charges might facilitate dimerization or aggregation of these peptides in aqueous solution, thereby leading to what would appear as high cooperativity in the curves.

Assessment of the CB_1 Receptor Juxtamembrane C-Terminal Conformation Using Peptide Fragments. The amphiphilic cationic nature of the $CB_1$401−417 peptide is reminiscent of mastoparan, a bee venom peptide that assumes a helical structure in a hydrophobic environment that is critical for its ability to activate G-proteins (*17*). Although it is theoretically predicted with molecular modeling parameters that this region of the CB_1 cannabinoid receptor can form an α-helix spontaneously (*9*), some structural limitations are expected due to the biological nature of this protein. As for a number of other G-protein coupled receptors, the juxtamembrane region of the CB_1 receptor possesses a Cys_{416} residue that is expected to be palmitoylated and would thereby tether the C-terminus to the membrane, forming a "fourth loop" (*18*−*20*). In the case of the CB_1 receptor, the structure imposed by Cys-palmitoyl anchoring to the membrane may be highly influential in receptor/G-protein coupling. In an attempt to determine the role of putative fourth loop anchoring to the membrane at Cys_{416}, the situation was mimicked by the loop peptide CB_1Cys401−415Cys (disulfide). The loop peptide attained 90% of the maximal activity as the peptide $CB_1$401−417 at a concentration of 1 mM, with an EC_{50} of 104 μM (Figure 5). A control for the additional Cys residues at either end of the peptide, CB_1-Cys(acm)401−415Cys(acm) was synthesized such that internal disulfide coupling or dimerization with other monomers would be prohibited. This blocked peptide suffered a loss of efficacy, attaining a maximal activity of 20% inhibition of adenylyl cyclase activity. The apparent affinity was similar to the loop peptide CB_1Cys401−415Cys (disulfide). It is possible that the acetamide groups on Cys residues, which would transform the properties of the termini from charged to hydrophobic, might be sufficient to alter the conformation that this peptide could achieve at the active site.

Structural Studies of Analogues of Peptide $CB_1$401−417. The CD spectra for peptide $CB_1$401−417 in water, sodium phosphate buffer, and methanol are characteristic of a random coil peptide (Figure 6A), having a weak maximum around 220 nm and a strong minimum around 198 nm (*21*). Minimal amounts of the anionic detergent SDS caused a definitive change in structure of $CB_1$401−417, having the most negative ellipticity at 222 nm and a dichroic spectra characteristic for peptide solutions having a high fractional population of residues in the α-helical conformation (*22*−*24*). An isodichroic point was present at 203 nm for SDS titration (data not shown), pointing to a clear transition to α-helical structure in SDS. The α-helical content was found to be almost independent of the amount of SDS in the range of 0.1−1%, indicating that the helical conformations are

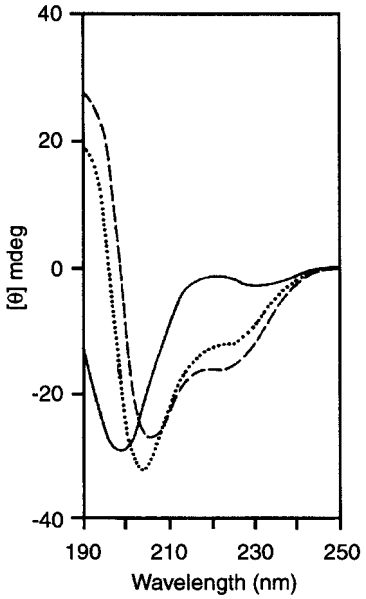

FIGURE 7: CD spectra for acetyl-Lys_{403}−$CB_1$401−417. Solvents were (—) 10 mM sodium phosphate, pH 7.2; (•••) 70% TFE; (− − −) 0.1% SDS.

stabilized within this range. Titrations with anionic lipid DPPG micelles also induced α-helical structure very similar to that of SDS: an isodichroic point was observed at 203 nm, indicating a clear transition to α-helical structure (data not shown). On the other hand, TFE titration indicated a random structure with a slight shift toward ordered structure (only a small hump appears around 222 nm) on addition of 90% TFE. This indicates that a hydrophobic environment does not induce α-helical structure in $CB_1$401−417. This is in contrast to mastoparan, for which α-helical structure was induced by methanol and TFE, as well as by SDS (Figure 6B).

CD spectra for acetyl-Lys_{403}−$CB_1$401−417 are shown in Figure 7, as determined in sodium phosphate buffer, 70% TFE, and 0.1% SDS. The acetyl-Lys_{403}−$CB_1$401−417 peptide remained random in sodium phosphate buffer, as is evident from an intensive negative band around 198 nm. Addition of TFE and SDS caused a drastic change in structure. A significant number of residues were in an α-helical conformation at 70% TFE. SDS induced α-helical structure at very small concentrations. SDS titration exhibited an isodichroic point at 203 nm (data not shown). DPPG micelles induced α-helical structure similar to SDS (data not shown). In comparison with $CB_1$401−417, the acetylated peptide is unique in that it assumes α-helical structure in a hydrophobic environment.

CD spectra for peptide $CB_1$402−417 recorded in sodium phosphate buffer and in various concentrations of TFE and SDS micelles are shown in Figure 8A. The spectrum was characteristic of random coil structure in sodium phosphate buffer, evident from the intense negative band around 198 nm. The TFE titration indicated a shift toward α-helical structure at 75% TFE, with a negative band appearing at 222 nm. At 90% TFE, some of the residues appeared to be in an α-helical conformation. SDS induced more α-helicity than TFE, evident from the appearance of negative bands around 208 and 222 nm. The α-helicity induced was less when the SDS concentration was below the critical micelle

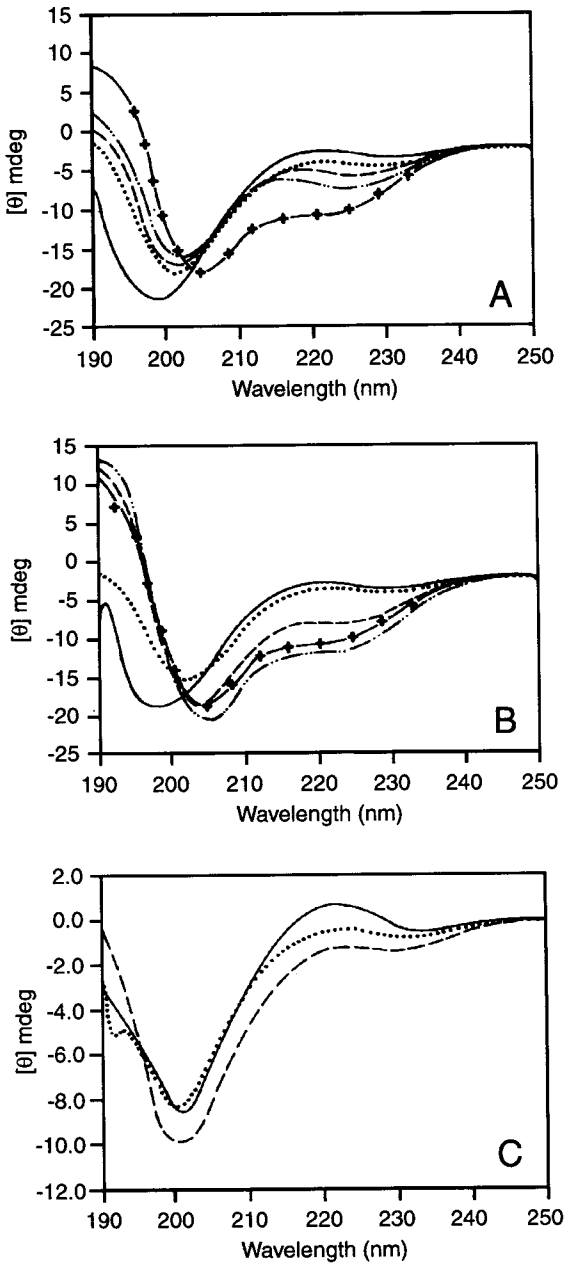

FIGURE 8: CD spectra for (A) $CB_1$402−417; (B) control CB_1 Cys(acm)401−415Cys(acm) peptide; and (C) the loop peptide CB_1 Cys401−415Cys (disulfide). Solvents for the peptides were (—) 10 mM sodium phosphate, pH 7.2; (•••) 25% TFE; (− − −) 75% TFE; (− •• −) 90% TFE; (+) 0.1% SDS in panel A or 0.5% SDS in panel B. In panel C the solvents were (•••) 10 mM sodium phosphate, pH 7.2; (− − −) 90% TFE; (—) 0.5% SDS.

concentration. The spectra seen in the presence of DPPG micelles were similar to those obtained in SDS, indicating induction of a significant amount of α-helical structure (data not shown).

CD spectra for peptide CB_1Cys(acm)401−415Cys(acm) are shown in Figure 8B. The peptide exists as a random coil structure in sodium phosphate buffer, as is evident from the intense negative band at 196 nm. TFE titration indicated the influence of a hydrophobic environment to induce α-helical structure. At 50% TFE, some shift toward helicity was initiated with a few residues in an α-helical conformation. Above 75% TFE, negative bands appeared around 208 and 222 nm and a positive band appeared around 192 nm. The

changes are characteristic for a gradual increase in the fractional population of residues in the helical conformation with increasing TFE concentration. There was an isodichroic point around 203 nm, indicating a clear transition to an α-helical conformation in the TFE hydrophobic environment. Studies performed in SDS and DPPG (data not shown) micelles also indicated induction of an α-helix, but the helicity induced was less than that in TFE.

CD spectra recorded for the loop peptide CB_1Cys401−415Cys (disulfide) in sodium phosphate buffer, TFE, and SDS are shown in Figure 8C. The peptide remained in a random coil structure in sodium phosphate buffer and in various concentrations of TFE, including 90% TFE. SDS titrations indicated the appearance of a positive band around 218 nm, a strong negative band around 198 nm, and a discernible band around 230 nm. This is characteristic of the presence of significant populations of residues in a PII conformation [poly(Pro) II helix] (*22*, *25*). The CD spectrum in the presence of DPPG micelles was inconsistent upon repetition, and so it could not be established convincingly whether the resulting PII conformation was greater or less than that seen with SDS. A PII conformation is a left-handed extended helix, in which contiguous residues are spaced by 3 Å along the helix axis, with three residues per helix turn. The ionized forms of the polypeptides poly(Lys) and poly(Glu) are the most documented examples of PII conformation in non-Pro-containing peptides (*21*, *25*).

In summary, all five peptides exist in a random coil conformation in aqueous solution, sodium phosphate buffer, and low concentrations of TFE. The anionic detergent SDS induces α-helix formation in all the peptide analogues except the loop peptide CB_1Cys401−415Cys (disulfide), where it induces a left-handed poly(Pro) II helical conformation. Considerable α-helical content was induced in all peptides except CB_1Cys401−415Cys (disulfide) by DPPG micelles. Among the set of peptides in which α-helix formation was induced, the amount of helical content increases progressively in the sequence CB_1Cys(acm)401−415Cys(acm) < CB_1-402−417 < acetyl-Lys_{403}−$CB_1$401−417 < $CB_1$401−417. This may be due to the higher probability of helix formation due to the Arg and Lys residues. In future studies, it will be of interest to identify the amino acid domain in which order is induced in these peptides.

DISCUSSION

Data presented previously (*10*) and in the present paper are consistent with the regulation of G_i by a peptide comprising the C-terminal juxtamembrane region of the CB_1 receptor. In more recent studies, we have demonstrated that the CB_1 receptor can be immunoprecipitated as a complex with G-proteins and that the peptide comprising the C-terminal juxtamembrane domain is able to disrupt this interaction in detergent solution (*11*). High concentrations of the peptide are required for this response, presumably due to the three-dimensional diffusion of peptide in detergent solution. Unfortunately, it is not possible to include high enough concentrations of the low-affinity peptide analogues described in the present paper to test their ability to directly compete for this interaction.

The efficacy of the CB_1 receptor juxtamembrane C-terminus peptide to activate G_i and G_o proteins suggests that the isolated peptide fragment can adopt a conformation mimicking that of the receptor. There are three Arg and one Lys nonconsecutive residues within the sequence of the CB_1 C-terminal peptide, posing the possibility for a cationic patch. For a number of G-protein coupled receptors, a motif of BBXXB or BBXB has been proposed to be present on the N-terminal domains of intracellular loops that couple to G-proteins (*15*, *16*). The cationic patch within the C-side of the third intracellular loop 15-mer peptide fragment from the 5-HT_{1A} receptor (*26*) results from a BBXXB motif. Studies of chimeric mutations of m_2/m_3-cholinergic receptors assayed for phosphatidylinositol-coupled Cl^- currents demonstrate that the G_q-selective region of the m_3-cholinergic receptor is the N-side intracellular loop 3 segment possessing the BBXB motif (*15*). The CB_1 receptor C-terminal peptide possesses a modification of such a motif (BXBXXB). It is possible that some flexibility exists regarding the importance of each basic amino acid in this motif. For example, a $G_{i/o}$ GTPase-activating peptide fragment from the α_{2A}-adrenergic receptor possesses a reversed BBXB motif (REKR) in addition to possessing a total of six basic amino acids (*27*). Ala scanning mutations of the C-side of the third intracellular loop sequence KKAAR within the m_1-cholinergic receptor suggest that the first basic residue could be modified, but the second and third are essential for coupling to G-proteins (*28*). The α_{2A}-adrenergic receptor C-side third intracellular loop/N-side third intracellular loop peptide dimer (coupled via a Cys−Cys disulfide bridge) potently stimulated GTPγS binding and GTPase activity (*29*). This dipeptide possesses a RWRGR sequence that, although charged, is not a motif that would be consistent with a patch of (+)-charged residues on one surface of an α-helix.

For the CB_1 receptor peptide studied here, loss of the first N-terminal positive charge (Arg_{401}) results in loss of affinity (see truncation and neutralization by Nle substitution). The loss of affinity by further truncation is minimal, suggesting that the high affinity is contributed primarily by the N-terminal Arg_{401}. Near-maximal activity is achieved by N-terminal truncated peptides, which possess fewer charged residues. The acetylation of Lys_{403} resulted in a 40% reduction of G-protein activation, which could be due either to the loss of the positive charge or to the addition of acetyl bulk to the peptide in this region. It is interesting to note that the juxtamembrane C-terminal region of the CB_1 receptor exhibits homology with the same region of the CB_2 receptor only on the N-terminal side of each peptide, for which the pattern RSKDLR in the CB_1 receptor is paralleled by RSGEIR in the CB_2 receptor. The CB_2 juxtamembrane peptide fragment failed to regulate G_i activity in this membrane assay (unpublished observations, S. Mukhopadhyay and A. C. Howlett), despite several conserved charged residues. These data would suggest that conferral of the G_i activation does not reside within the highly charged residues located at the N-terminal region of the peptide. The single charged residue on the C-terminal side of $CB_1$401−417, Glu_{417}, can be truncated or neutralized by Leu substitution with some loss of activity. It can be hypothesized that the highly charged N-terminus may be required for docking at the site of action, and the C-terminal negatively charged residue may participate in this action.

Lechleiter and colleagues (*15*) suggested that a common feature found among receptors that couple to G_q (m_1-, m_3-,

and m_5 -cholinergic, $5HT_{1C}$ and $5HT_{2B}$, and α_{1A}-adrenergic receptors) appears to be a "region of potentially amphipathic, α-helix followed by a somewhat hydrophobic sequence as proposed for mastoparan." An amphiphilic helical structure has been shown for the C-side of the third intracellular loop 15-mer peptide fragment from the $5\text{-}HT_{1A}$ receptor (*26*). This peptide interacts with G_i to inhibit forskolin-stimulated adenylyl cyclase in cell membrane fractions. CD polarimetry of this peptide in TFE (but not sodium phosphate buffer) indicates α-helicity as predicted for an amphiphilic cytoplasmic extension of transmembrane α-helix. The amphiphilic cationic nature of the CB_1 C-terminal juxtamembrane peptide suggests that α-helical structure could be induced in certain environments. However, according to its CD spectrum, peptide $CB_1401-417$ exists in aqueous solution as an unstructured peptide, and this random coil persists in a hydrophobic environment. One can postulate that the reason that the Arg_{401} truncated $CB_1402-417$, the acetamide-blocked CB_1Cys(acm)401−415Cys(acm), and the acetylated acetyl-$Lys_{403}-CB_1401-417$ peptides exhibit some α-helix formation in 90% TFE is that the N-terminal negative charges play a role in restricting α-helix formation in a hydrophobic environment. These peptides could develop α-helical structure in SDS, which suggests that the positively charged residues must be stabilized in an α-helical structure by the negatively charged SDS.

In the biological mechanism of G_i activation, the receptor domain could be in an unstructured form as it interacts with the G-protein. To mimic this conformation, the juxtamembrane C-terminal peptide may form a looped structure stabilized by the docking site at Arg_{401} and facilitated by a charge interaction of the C-terminal Glu_{417} and a positively charged residue, probably Arg_{401}, at the N-terminal side of the peptide. Alternatively, the receptor domain could be α-helical as it interacts with the G-protein. To mimic this conformation, a negatively charged region on the G-protein surface could stabilize an α-helical structure of the peptide as it binds to the G-protein surface. To address these two alternatives, we created a peptide possessing Cys residues at the terminal ends and coupled the ends by a disulfide linkage. This loop peptide remains unstructured in both aqueous and hydrophobic environments and forms a PII left-handed helix in the presence of SDS. This loop peptide exhibits full ability to activate G_i and suffers only a 3-fold loss of apparent affinity for the G-protein. In contrast, the control peptide, possessing blocked Cys residues at both ends, is able to form α-helical structure in a hydrophobic environment, perhaps as the result of occluded charges at the terminal ends of the peptide. This blocked peptide exhibits incomplete ($<50\%$) activation of G_i and suffers a 4-fold loss of affinity for the G-protein. Thus, the ability to form α-helical structure is not requisite to activation of G_i by these peptides. Although we could predict that peptide $CB_1401-417$ would form α-helical structure stabilized by an interaction with negatively charged phospholipid headgroups (e.g., phosphatidic acid) at the membrane surface, such conditions may not be optimal for peptide interaction with the G-protein surface. Freissmuth and colleagues (*30*) have studied the structures and biological properties of peptides representing the domains of GPCRs that activate G-proteins. Their findings conclude that an amphipathic α-helical structure of the charged motif is not requisite to a productive interaction with G-proteins (*30*).

The present studies have specifically addressed charge and helicity within the peptide simulating the C-terminal juxtamembrane region of the CB_1 receptor. There are other aspects of this region of the molecule that remain to be addressed. The three Ser residues (Ser_{402}, Ser_{411}, and Ser_{415}) are possible targets of phosphorylation/dephosphorylation reactions. Should one or more of these residues serve as substrates for protein kinases, the charge distribution along this region of the receptor would be modified by inclusion of negative charges. The influence of these negative charges on the conformation of the receptor remains to be addressed. Conversely, the formation of an α-helical structure in this region may influence the availability of one or more of these Ser residues to serve as substrates for protein kinases. Also not addressed in these studies is the role of Pro_{414} as a potential helix-breaker, demarcating the potential termination of an α-helical domain and origin of a random coil. The substitution of polar or charged amino acids for those hydrophobic residues that predict helicity within this domain of the receptor (Leu_{405}, Ala_{408}, Phe_{409}, Met_{412}, Phe_{413}) has not been addressed. Although the present studies suggest that α-helical structure is not necessary for function, assessed as inhibition of adenylyl cyclase, α-helicity may be important for other aspects of receptor regulation. If potential regulatory aspects of α-helical structure are identified, then modifications of these residues will be warranted. Importantly, the influence of palmitoylation of Cys_{416} remains to be addressed. Preliminary studies in our laboratory have indicated that $>95\%$ of immunoprecipitatable CB_1 cannabinoid receptors in rat brain membranes are palmitoylated (unpublished observations, S. Mukhopadhyay and A. C. Howlett). One might predict that palmitoylation/depalmitoylation reactions would influence the conformation of the juxtamembrane C-terminal region in a physiologically relevant way. These questions remain to be addressed by more extensive comprehensive investigations of phosphorylation and palmitoylation as regulatory mechanisms for CB_1 receptor signaling.

One might question the ability of an isolated peptide to adequately simulate the domain found within the optimally folded protein as it exists in its native membrane environment. Membrane surface is considered to comprise three layered compartments: a hydrophobic, an aqueous suface, and an aqueous bulk compartment (*31*). Because of the presence of anionic lipids in biological membranes, there is a negative surface potential near the interface. This negative surface potential is diffusive and decreases with distance from the fixed charges and increasing ionic strength of the surrounding medium. Sargent and Schwyzer (*32*) suggested that catalysis of ligand−receptor interactions is an important function of the lipid phase of the cell membrane. In their model, a direct ligand−receptor reaction is replaced by multiple sequential steps including (i) surface accumulation of charged ligands; (ii) ligand-membrane interactions; and, ultimately, (iii) binding to the receptor itself. Applying this model to the present data, activation of G-proteins by these peptides may be mediated through the following four steps: (i) the solution conformation of the peptide; (ii) an electrostatic interaction of the peptide with the lipid headgroups of the membrane, with Arg_{401} playing a prominent role; (iii) a hydrophobic interaction of the peptide in the lipid acyl chains; and (iv) the G-protein bound state. In the intact functional CB_1 receptor, such a sequence of events may be

replaced by conformational changes induced by agonist binding that may subserve the intervening steps to catalyze the conversion of the C-terminal juxtamembrane domain from the inactive conformation to the G-protein-activating state. We have shown that peptide $CB_1$401−417 is able to compete for CB_1 receptor−G-protein association in detergent solution (*11*), indicating that the peptide can interact with G-proteins at a receptor-binding site. It will be of interest to continue these studies by determining where the peptide interaction site resides on the G-proteins and what the mechanism is for activation by the peptide.

ACKNOWLEDGMENT

We thank Ms. Jill Pigg and Ms. Kelly Jester for cell culture maintenance and membrane preparations. We also thank Dr. Michael Shuie at Princeton Biomolecules and Dr. Jung Huang at Saint Louis University for helpful discussion regarding peptide modifications. We gratefully acknowledge Dr. Ned Seigel and Ms. Jennifer Wong at Monsanto Corp. for helpful advice and the use of their CD spectropolarimeter for some of these studies.

REFERENCES

1. Howlett, A. C. (1985) *Mol. Pharmacol. 27*, 429−436.
2. Pacheco, M., Childers, S. R., Arnold, R., Casiano, F., and Ward, S. J. (1991) *J. Pharmacol. Exp. Ther. 257*, 170−183.
3. Mackie, K., and Hille, B. (1992) *Proc. Natl. Acad. Sci. U.S.A. 89*, 3825−3829.
4. Bouaboula, M., Bourrié, B., Rinaldi-Carmona, M., Shire, D., LeFur, G., and Casellas, P. (1995) *J. Biol. Chem. 270*, 13973−13980.
5. Gerard, C., Mollereau, C., Vassart, G., and Parmentier, M. (1990) *Nucleic Acids Res. 18*, 7142.
6. Matsuda, L. A., Lolait, S. J., Brownstein, M. J., Young, A. C., and Bonner, T. I. (1990) *Nature 346*, 561−564.
7. Chakrabarti, A., Onaivi, E. S., and Chaudhuri, G. (1995) *DNA Seq.- J. Seq. Map. 5*, 385−388.
8. Abood, M. E., Ditto, K. E., Noel, M. A., Showalter, V. M., and Tao, Q. (1996) *Biochem. Pharmacol. 53*, 207−214.
9. Bramblett, R. D., Panu, A. M., Ballesteros, J. A., and Reggio, P. H. (1995) *Life Sci. 56*, 1971−1982.
10. Howlett, A. C., Song, C., Berglund, B. A., Wilken, G. H., and Pigg, J. J. (1998) *Mol. Pharmacol. 53*, 504−510.
11. Mukhopadhyay, S., and Howlett, A. C. (1998) *Mol. Biol. Cell 9*, 121a.
12. Shen, S., and Strobel, H. W. (1993) *Arch. Biochem. Biophys. 304*, 257−265.
13. Chin, C. N., Lucas-Lenard, J., Abadji, V., and Kendall, D. A. (1998) *J. Neurochem. 70*, 366−373.
14. Rinaldi-Carmona, M., Barth, F., Heaulme, M., Alonso, R., Shire, D., Congy, C., Soubrie, P., Breliere, J.-C., and LeFur, G. (1995) *Life Sci. 56*, 1941−1947.
15. Lechleiter, J., Hellmiss, R., Duerson, K., Ennulat, D., David, N., Clapham, D., and Peralta, E. (1990) *EMBO J. 9*, 4381−4390.
16. Okamoto, T., and Nishimoto, I. (1992) *J. Biol. Chem. 267*, 8342−8346.
17. Higashijima, T., Burnier, J., and Ross, E. M. (1990) *J. Biol. Chem. 265*, 14176−14186.
18. Ovchinnikov, Y., Abdulaev, N., and Bogachuk, A. (1988) *FEBS Lett. 230*, 1−5.
19. Kennedy, M. E., and Limbird, L. E. (1993) *J. Biol. Chem. 268*, 8003−8011.
20. O'Dowd, B. F., Hnatowich, M., Caron, M. G., Lefkowitz, R. J., and Bouvier, M. (1989) *J. Biol. Chem. 264*, 7564−7569.
21. Woody, R. W. (1995) *Methods Enzymol. 246*, 34−71.
22. Woody, R. W. (1992) *Adv. Biophys. Chem. 2*, 37−79.
23. Johnson, C. W. J. (1988) *Annu. Rev. Biophys. Biomol. Struct. 17*, 145.
24. Brahms, S., and Brahms, J. (1980) *J. Mol. Biol. 138*, 149−178.
25. Sreerama, N., and Woody, R. W. (1994) *Biochemistry 33*, 10022−10025.
26. Varrault, A., Nguyen, D., McClue, S., Harris, B., Jouin, P., and Bockaert, J. (1994) *J. Biol. Chem. 269*, 16720−16725.
27. Wade, S. M., Dalman, H. M., Yang, S.-Z., and Neubig, R. R. (1994) *Mol. Pharmacol. 45*, 1191−1197.
28. Lee, N., Geoghagen, N., Cheng, E., Cline, R., and Fraser, C. (1996) *Mol. Pharmacol. 50*, 140−148.
29. Wade, S. M., Scribner, M. K., Dalman, H. M., Taylor, J. M., and Neubig, R. R. (1996) *Mol. Pharmacol. 50*, 351−358.
30. Voss, T., Wallner, E., Czernilofsky, A. P., and Freissmuth, M. (1993) *J. Biol. Chem. 268*, 4637−4642.
31. Schwyzer, R. (1991) *Biopolymers 31*, 785−792.
32. Sargent, D. F., and Schwyzer, R. (1986) *Proc. Natl. Acad. Sci. U.S.A. 83*, 5774−5778.

BI981767V